*https://doi.org/10.46813/2024-150-101*

UDC 621.793.74:669.094.54

# INFLUENCE OF THE METAL UNDERLAYER ON THE CAVITATION RESISTANCE OF NITRIDED STEEL WITH $Mo_2N$ COATING

*Yu.A. Zadneprovskiy[1], V.A. Belous[1], I.S. Domnich[1], V.I. Kovalenko[1], H.Yu. Rostova[1], I.G. Tantsyura[1], G.N. Tolmachova[1], M.G. Ishchenko[2], A.S. Kuprin[1]*
*[1]National Science Center "Kharkov Institute of Physics and Technology", Kharkiv, Ukraine;*
*[2]JSC "Ukrainian Energy Machines", Kharkiv, Ukraine*
*E-mail: yaz@kipt.kharkov.ua*

A complex modification of 25CrMoV steel has been carried out, which includes nitriding in arc-enhanced glow discharge plasma, deposition of metallic sublayer (Mo, Cr or Ti) and deposition of top layer of $Mo_2N$ coating. The structure studies showed that depending on the material and the thickness of the sublayer (1.5...6 μm), defects and delaminations could form at the interfaces, while no defects were observed in the absence of the metallic sublayer. The concentration of nitrogen in the complex modified layers depends on the composition of the metallic sublayer, but does not affect the total depth of nitriding of the hardened steel ~ 160 μm. The hardness of the nitrided layer is ~ 12 GPa, and the hardness of the $Mo_2N$ coating is ~ 30 GPa. The cavitation resistance of complex-modified 25CrMoV steel without the metal sublayer is 2 times higher than the initial steel.

## INTRODUCTION

The advantages of the technology of complex surface modification of structural materials [1, 2] include additional increase of their operational properties by means of gradual surface modification by various methods of physical vapor deposition (PVD). For example, in order to increase the service life of steel parts of steam distribution and control mechanisms of turbines of thermal power plants, a complex ion-plasma treatment was used, in which the working surfaces of the parts were subjected to ion nitriding, followed by the deposition of protective coatings [3].

Diffusion penetration of activated nitrogen during ion plasma nitriding takes place deep into the surface of the steel heated to the optimum temperature [4]. Nitrogen activation can be performed in the working volume of an arc enhanced glow discharge (AEGD) [5]. In this case, activated high-energy nitrogen atoms diffuse into the steel to the highest depths [6]. The efficiency of nitriding can be determined by a parameter such as the depth of hardening of the steel. The deposition of hard nitride layers, e.g. $Mo_2N$, makes it possible to obtain an outer wear-resistant layer [7].

Thus, the complex ion-plasma hardening process achieves multilayer surface protection, each layer of which has both specified strength and functional properties, such as anti-corrosion, anti-abrasion or anti-cavitation [8]. It is important to achieve a high level of interlayer strength of the modified microstructures. As a result, the service life of working surfaces of parts and units used in various areas of mechanical engineering is increased many times over.

To increase the adhesion properties of protective hard coatings to the modified surface during PVD deposition, transition layers of different metals are traditionally used [9]. Intermediate metal layers can also be used to provide the required properties of the main functional layer within the multilayer structure. For example, bombardment of the surface of nitrided steel with accelerated titanium ions at energies up to 1.5 keV resulted in the formation of a surface layer based on $TiN_x$ nitride [10], which prevents back diffusion of nitrogen from the steel.

The use of standard vacuum-arc equipment for complex ion-plasma hardening of parts makes it possible to clean the working surface of the part by ion sputtering, its heating prior to the nitriding stage by means of energetic bombardment with metal ions. Characteristics of the influence of surface preheating on the nitriding depth are presented in the publication [11].

The aim of the present work is to investigate the structure, nitrogen concentration profiles, hardness and cavitation resistance of modified layers of 25CrMoV steel depending on the composition and thickness of intermediate layers of metal coatings.

## 1. MATERIALS AND EXPERIMENTAL METHODS

Samples for research with the dimensions of 20×10×6 mm were made of 25CrMoV steel (standard No. 20072-74). Complex ion-plasma modification was performed on a Bulat type vacuum arc machine additionally equipped with AEGD. Processing parameters are described in [11].

The complex ion-plasma surface modification of 25CrMoV steel consisted of three steps:

– Nitriding in AEGD at temperature ~ 600 °C, $P_{N2}$ = 0.3 Pa, t = 40 min;

– Deposition of a metallic sublayer (Me: Mo, Cr or Ti with thickness from 0 to 6 μm) by vacuum arc method at bias potential -50 V and pressure 0.0027 Pa, T = 500 °C;

– deposition of $Mo_2N$ nitride layer (thickness 10 μm) by vacuum arc method at bias potential -70 V and nitrogen pressure 0.27 Pa, T = 450 °C.

The microstructure of the modified layers was studied on cross-sections of steel samples using an Olympus GX51 inversion metallographic microscope. Nitrogen distribution profiles in complex modified layers (coatings and steel) were obtained using a JSM

7000-1F scanning electron microscope equipped with X-ray energy dispersive microanalysis. Hardness (H, GPa) and Young 's modulus (E, GPa) profiles were measured using a G200 nanoindenter equipped with a Berkovich indenter. Indentation was performed along the cross section of the specimen with indenter penetration depths of ~ 200 nm.

Cavitation wear tests on samples with complex surface modifications were carried out on a special device [12]. The device was an ultrasonic generator that provided oscillations of the emitter at a frequency of 20 kHz. In water, a cavitation zone is created under the end of the emitter, resulting in erosion of the sample surface. The diameter of the eroded zone on the surface of the samples in these studies was approximately 7 mm. The degree of coating destruction was determined by weight loss (Δ m, mg) as a function of cavitation exposure time (t, h). Zones of surface erosion after cavitation were studied using an optical microscope.

## 2. RESULTS AND DISCUSSION

Fig. 1 shows images of the microstructure of complex modified layers with an intermediate Mo layer of different thicknesses. Each of the images in Fig. 1 shows (from left to right): the nitrided steel layer, the Mo sublayer (see except Fig. 1,a), and the outer $Mo_2N$ coating layer.

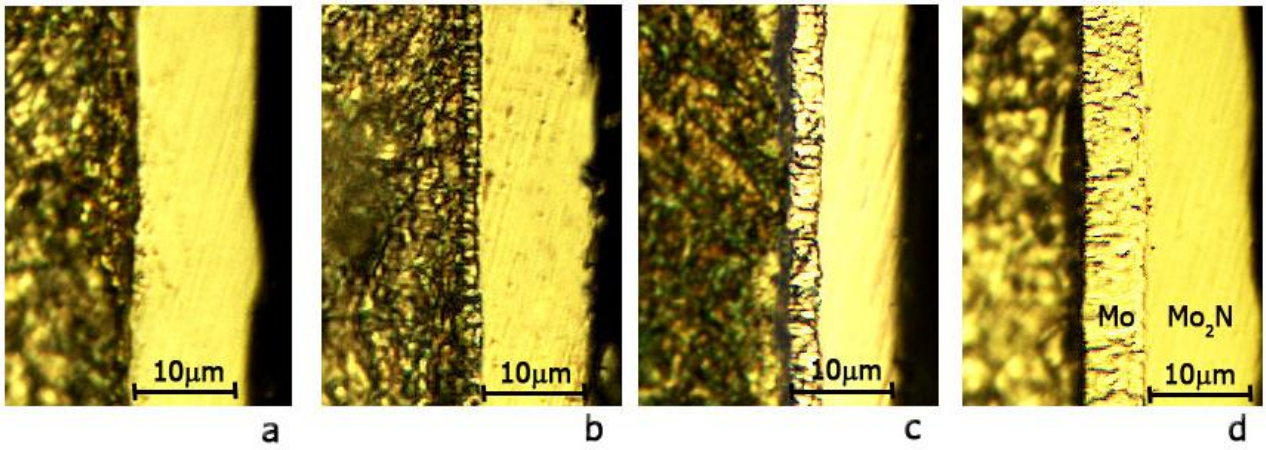


*Fig. 1. Optical images of the structure of nitrided steel with $Mo_2N$ coating (a) and Mo sublayer with thickness of 1.5 (b); 3 (c) and 6 μm (d)*

The microstructure of the molybdenum sublayer has the characteristics of columnar with grain growth perpendicular to the surface of the steel substrate (see Fig. 1,b,c,d). In all images, the transition zones between the molybdenum layer and the outer molybdenum nitride are observed to be quite dense with no delamination or other visible defects. However, in the transition zones between the nitrided steel and the Mo coating, areas of voids are visible along the steel-coating interface (see Fig. 1,a). The same defect is observed between the steel surface and the 3 μm Mo layer in Fig. 1,c. In Fig. 1,d for the 6 μm layer, a wider area of voids can be seen in the same region. In general, as can be seen from the micrographs, there is a tendency for the number of defects in the transition zone between the steel surface and the Mo coating to increase as a function of increasing the thickness of the Mo sublayer. The exception is the transition zone between layers with 1.5 μm Mo sublayer (see Fig. 1,b). From a defect-free point of view, this sublayer thickness may be optimal.

Fig. 2 shows images of the microstructure of the complex-modified layers obtained from cross-sections of the samples, with Ti sublayers of different thickness.

It can be seen (see Fig. 2) that the Ti sublayers as well as the Mo sublayers (see Fig. 1) have a similar columnar structure. The transition between the Ti layer and the outer $Mo_2N$ layer is also (as for the Mo layer) defect-free. No such delaminations are observed between the Ti layer and the nitrided surface as observed for the Mo layer. The structure of the Cr layer is similar to that of the Ti layer, and the structures of the transition zones between the layers are also similar, so additional images are not shown.

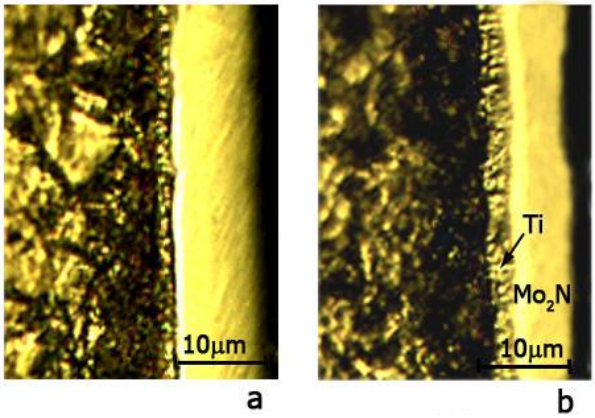


*Fig. 2. Optical images of the structure of nitrided steel with $Mo_2N$ coating and Ti sublayer thickness: 1.5 (a) and 3 μm (b)*

The structure of molybdenum nitride coating is γ-$Mo_2N$ with lattice parameter a = 0.420 and crystallite size ≈ 11 nm [3].

Fig. 3 shows the distribution curves of nitrogen concentration in the surface layers of complex modified steel 25CrMoV.

As can be seen from Fig. 3, the differences in the values of nitrogen concentrations in the coatings (to the left of the vertical line) ~ 35 (1, 2) and ~ 55 at.% (3) are

due to their different compositions: Mo (1, 2) and $Mo_2N$ (3).

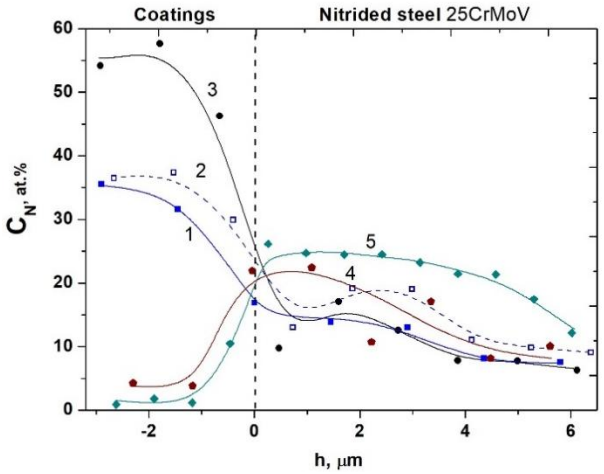


*Fig. 3. Distribution of nitrogen concentration on cross sections of samples obtained by complex modification with Mo (1, 2), Cr (4), and Ti (5) sublayers. Sublayer thickness: 0 (3); 3 (1, 4, 5), 6 μm (2) (the vertical line indicates the surface of the nitrided steel)*

The nitrogen concentration in the Mo sublayer is quite high ~ 35 at.%. In the near-surface zone of the nitrided steel (to the right of the vertical line), a decrease in the distribution curves and a small maximum are observed. In addition, the distribution curve of nitrogen (2) with a thicker Mo sublayer ($h_{Mo}$ = 6 μm) is slightly higher. The value of the nitrogen concentration in the Mo sublayer does not depend on its thickness. The saturation of molybdenum sublayers with nitrogen apparently occurs to a greater extent from the side of the $Mo_2N$ deposition zone. The decrease of the nitrogen concentration on the curves is explained by the bombardment of the nitrided steel surface by heavy Mo ions, which leads to a decrease of its concentration in thin layers ($h \leq 1.5$ μm). The maximum nitrogen concentration of ~ 20 at% observed in curve (2) for the sample with a molybdenum sublayer ($h_{Mo}$ = 6 μm) is due to the redistribution of nitrogen from the near surface region to the depth of the steel. This is due to longer term temperature effects on the nitrided surface.

For nitrided samples with Cr or Ti sublayers and $Mo_2N$ outer coatings, the nitrogen concentration distribution (see Fig. 3, curves (4) and (5)) is generally similar. The difference between these curves is the higher nitrogen concentration (curve 5, Ti sublayer), which has a value of more than 20 at% at a distance of 0.5 to 5 μm from the surface of the nitrided steel. At the same time, a low nitrogen concentration is observed in the Ti and Cr sublayers: $C_N$ ~ 1.5 at.% (curve 5) for Ti, and $C_N$ ~ 4 at.% (curve 4) for Cr. There is no nitrogen-depleted zone in the near-surface region of the nitrided steel (curves 4, 5).

The low concentration of nitrogen in the Cr and Ti sublayers can be explained by the fact that nitrogen, which has a greater chemical affinity for titanium and chromium than for molybdenum, forms thin nitride compounds ($Ti_xN$ and $Cr_xN$) along both boundaries of the layers of these metals. Due to the low mobility of nitrogen in these compounds, nitrogen penetration into the depth of the layers is blocked, both from the $Mo_2N$ coating condensation zone and from the nitrided steel. The bombardment of the surface of the nitrided steel with Cr and Ti ions, which are lighter than Mo, in the process of deposition of the metal sublayer does not cause back diffusion of nitrogen.

To evaluate the interlayer strength characteristics and to determine the relationship between the nature of the distributions of nitrogen concentrations and hardnesses, the hardness profiles in the modified layers were investigated (Fig. 4).

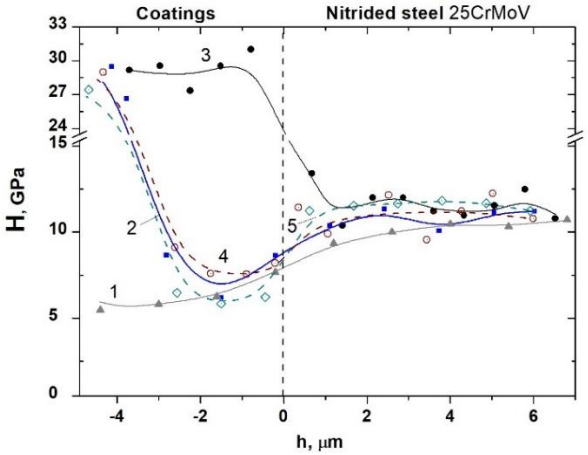


*Fig. 4. Hardness distribution along the cross section of complexly modified samples with sublayers of Mo (1, 2), Cr (4), and Ti (5) with a thickness: 0 (3); 3 (2, 4, and 5), 6 μm (1)*

From Fig. 4 it can be seen that the two hardness curves (1 and 2) of the samples with complex modification and Mo sublayer have a similar character to the right of the nitrided steel surface, and the differences in the course of these curves are observed in the area of the Mo coating (to the left of the vertical line) and are due to the different thickness of these layers. The hardness value of the Mo coating is ~ 6 GPa (see Fig. 4, curves 1 and 2). To the right of the vertical line, in the near-surface nitrided region, the hardness has an average value of 11.5 GPa, which corresponds to high values after nitriding for 25CrMoV steel. Curve (3), which refers to the hardness distribution in the sample without sublayer deposition, looks different. To the left of the vertical line, in the region of the $Mo_2N$ layer, it has a plateau shape, the values of which correspond to the hardness level of this layer ~ 30 GPa. Then, in the transition region between molybdenum nitride and nitrided steel, there is a sharp drop in hardness to the hardness values of nitrided steel ~ 12 GPa. This hardness profile correlates well with the nitrogen distribution profile for the sample with the corresponding complex treatment (without interlayer) shown in Fig. 3 (curve 3).

The hardness distributions with Cr and Ti sublayers (h = 3 μm), both in the sublayer coating and in the near-surface region of the nitrided steel, are the same (see Fig. 4, curves 4 and 5). However, the hardness levels in the Cr and Ti sublayers (see Fig. 4) are different: for the Cr layer, the average hardness value is ~ 7.5 GPa, while for the Ti layer it is ~ 6 GPa. In the near-surface nitrided region: with the Cr sublayer deposited on its surface, the hardness is about 11 GPa, and for the Ti sublayer it is

higher and is about 12 GPa. Moreover, both the type of distribution of hardness profiles for these samples and their values correlate with the distributions of nitrogen concentration in (see Fig. 3).

25CrMoV steel contains mainly the following metals: Cr (up to 1%), small additions of Mo and Ti (< 1%), Fe – balanced. Small additions of titanium also diffuse into its surface during the deposition of Ti sublayer [13]. According to [14], metal alloying elements such as Ti dissolved in ferrite contribute to the increase of nitrogen solubility in the α-Fe phase due to the high activity of titanium to combine with nitrogen. Thus, in the presence of a sufficient concentration of nitrogen in the surface layer of the steel, combined with the necessary temperature, as in this case, the formation of $Fe_xN$, $Cr_xN$ and $Ti_xN$ compounds occurs.

Hardness distributions in nitrided steel obtained by complex treatment with deposition of different compositions of metal sublayers are shown in Fig. 5. It can be seen that the character of the hardness profile distribution in nitrided steel does not differ practically, and the hardening depths for all samples are equal and make up to 160 μm (see Fig. 5). Thus, different composition of metal sublayers used in complex modification does not affect the overall hardening depth of nitrided steel.

The deposition of metallic sublayers only affects the hardness distribution in the transition and near-surface regions of nitrided steel, which may affect the interlayer strength of the complex surface modification as a whole.

To determine the effect of the deposition of various metallic sublayers on the strength properties of the complex modified surface, cavitation tests were performed on the samples.

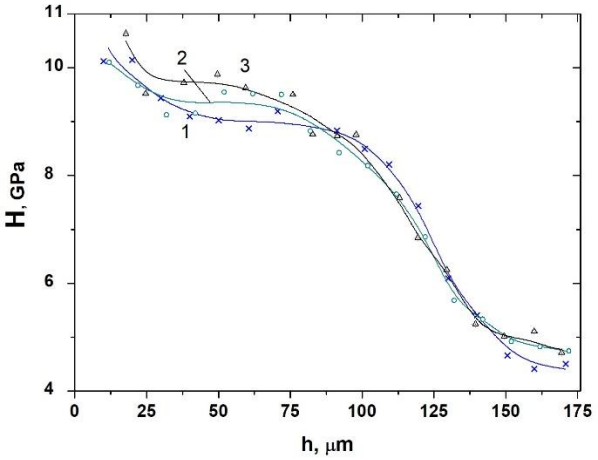


*Fig. 5. Hardness profiles of complex-modified nitrided steel samples with sublayers: Mo (1), Ti (2), and no Me sublayer (3). The thickness of the layers is 3 μm*

The kinetic curves of cavitation wear of samples with complex modification and Me (Mo, Cr, and Ti) sublayers are shown in Fig. 6.

The weight loss of the complex-modified samples without the sublayer and with its small thickness (see Fig. 6, curves 1–5) for 6 h of testing is approximately twice the weight loss of the untreated steel (see Fig. 6, curve 7). This indicates the high wear resistance of the modified surfaces. Complex modified samples with thicker interlayer (see Fig. 6, curves 5 and 6) have slightly lower resistance than samples with thinner interlayer (see Fig. 6, curves 2 and 4). The result indicates that the resistance does not depend much on the material of the interlayer (molybdenum or chromium).

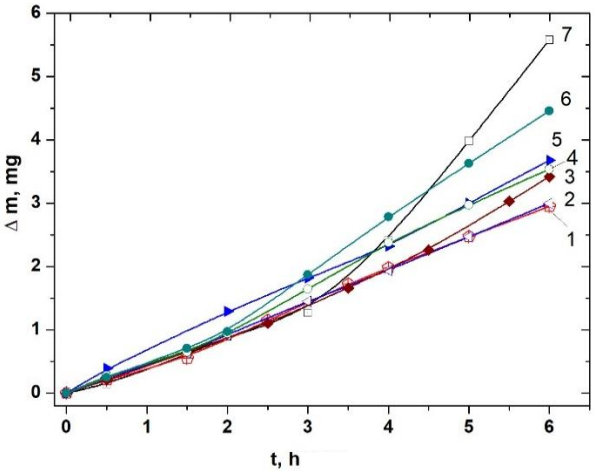


*Fig. 6. Weight loss of the initial 25CrMoV steel sample (7), samples without Mo sublayer (1) and with Mo (2 and 5), Cr (3), and Ti (4 and 6) sublayers as a function of cavitation test time. Sublayer thickness: h = 1.5 (2 and 4), 3 μm (3, 5, and 6)*

The weight loss for the sample with Ti sublayer (see Fig. 6, curve 4) at its thickness of 1.5 μm, based on the results of 6-hour tests, is equal to the weight loss for the sample with Mo sublayer at its thickness of 3 μm (see Fig. 6, curve 5). The weight loss for the specimen with the Ti sublayer with a greater thickness of 3 μm (see Fig. 6, curve 6) is even greater. As a result, the cavitation wear of the $Mo_2N$ layer for the complex modification with Ti sublayer is higher than that for the modification with Mo sublayer.

The surface images of complex-modified steel samples with different thicknesses of metal sublayer after 6 h of cavitation testing are shown in Fig. 7. It can be seen that for the original steel sample, the surface wear is uniform in area (see Fig. 7,a). The complex hardened samples (see Fig. 7,b,d,f,g) are characterized by pitting wear that occurs where macroparticles of cathode material are embedded [15]. As can be seen from the figure, the number of pitting failures increases with the thickness of the sublayer (see Fig. 7,f,g). The lowest number of craters on the surface is found in samples without a sublayer and with a minimum sublayer thickness of 1.5 μm (see Fig. 7,d,b). No dependence of the number of pits on the sublayer material (molybdenum or chromium) was observed.

The mechanism causing such fractures is due to the microshock effect of cavitation bubbles, which leads to pressure on the surface areas of the sample and its vibration and deformation [16, 17]. It should be noted that in the multilayer structure there is a softer metal sublayer under the hard molybdenum nitride coating. Therefore, samples with a thicker metal sublayer will experience more vibration of the outer $Mo_2N$ layer. In addition, molybdenum nitride is characterized by high internal stress, which makes it quite brittle [3, 18]. These factors contribute to the formation of

microcracks, and with increasing test time, these coating defects experience increased erosion into the depth of the material. Complex-modified samples without metal coating lack a soft layer and the process of microcrack formation is slower.

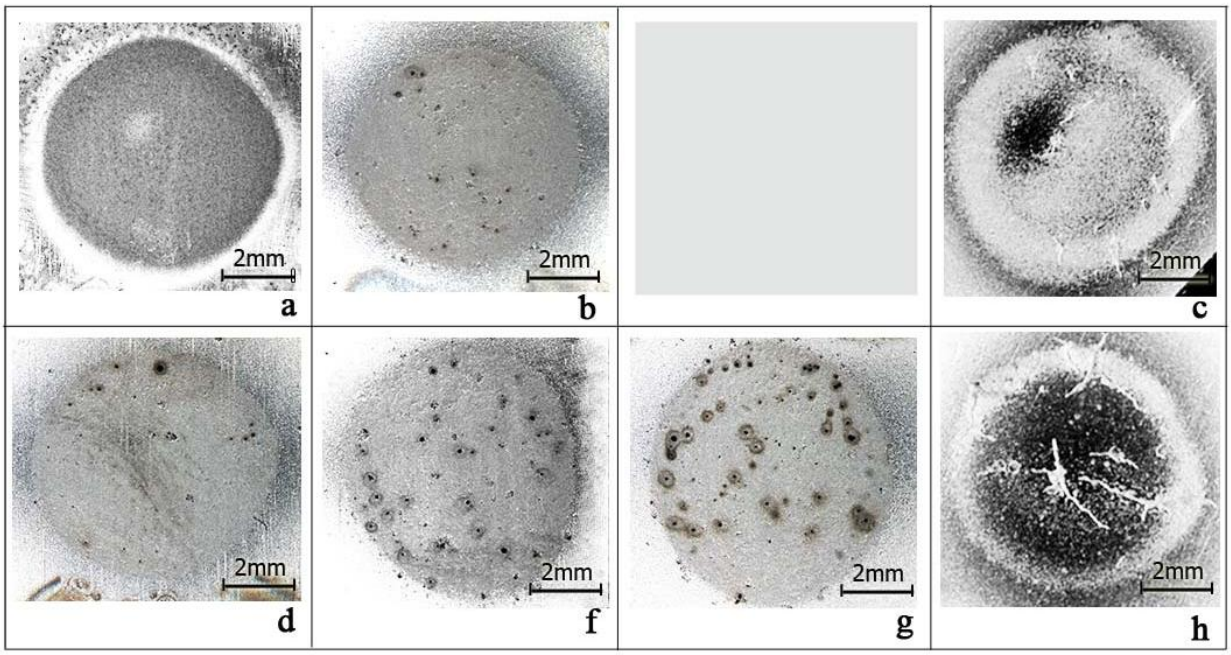


*Fig. 7. Surface images of samples after cavitation test: initial (a); complex modified without sublayer (d) and with deposition of Mo (b and f), Cr (g) and Ti sublayers (c and h). Sublayer thickness: h = 1.5 (b and c), 3 μm (f, g, and h)*

The character of defects on the surface of $Mo_2N$ coating with Ti sublayer after cavitation action is different from that of samples with Mo and Cr sublayers, as can be seen from Fig. 7,c,h. Defects in the form of "star cracks" are observed on the surface of the $Mo_2N$ coating. Moreover, for the 1.5 μm sublayer (see Fig. 7,c), these are single local "stars" and for the 3 μm sublayer (see Fig. 7,h), they are longer (2…3 mm) cracks.

The differences in the type of damage to the $Mo_2N$ coating surface depending on the material of the sublayers (Mo, Cr or Ti) can be explained by their different physical and mechanical properties. In addition to the sublayer hardness, the cavitation resistance of the system can be influenced by the difference in Young's modulus of the steel substrate, the metal sublayer and the top nitride layer [19, 20]. The Young's modulus values (E, GPa) for the Mo and Cr sublayers were similar and are ~ 340 GPa, while for the Ti layer they are ~ 150 GPa, for the nitrided steel ~ 250 GPa, and for the $Mo_2N$ coating ~ 420 GPa. Thus, the Ti sublayer material has a lower Young's modulus than the other treatments, which results in the lower cavitation resistance of the $Mo_2N$ coating.

To improve the cavitation resistance of complex modified steel, metals with high Young's modulus, such as Mo, should be selected for the sublayer material, and the thickness of the metal layers should not exceed 1.5 μm.

## CONCLUSIONS

A complex modification of 25CrMoV steel was performed, including nitriding in arc-enhanced glow discharge plasma, deposition of metallic sublayers (Mo, Cr or Ti) and deposition of a top layer of $Mo_2N$ coating. The structure, composition, and mechanical properties of the modified samples were investigated:

1. Depending on the material and thickness of the sublayer, defects and delaminations may form at the interfaces. There are no defects in the structure without a metallic sublayer.

2. Nitrogen distribution in complex modified layers depends on the composition of the metal sublayer. The presence of a Mo sublayer can cause nitrogen redistribution in the steel surface, while Cr and Ti sublayers have no such effect.

3. The deposition of metallic sublayers during complex modification affects the hardness distribution in the transition and near-surface regions of nitrided steel, but does not affect the overall hardening depth (~ 160 μm) of nitrided steel.

4. The hardness of the nitrided steel is ~ 12 GPa and the hardness of the $Mo_2N$ coating is ~ 30 GPa for the complex-modified samples without sublayer.

5. The cavitation resistance of complex-modified steel 25CrMoV without a metal sublayer is 2 times higher than that of the steel in the initial state. The presence of the metal sublayer leads to a decrease in the cavitation resistance of the $Mo_2N$ coating, the lower its Young's modulus and the greater its thickness.

## ACKNOWLEDGEMENT

The work was financially supported by the National Academy of Science of Ukraine (program "Support of the development of main lines of scientific investigations" (KPKVK 6541230)).

## REFERENCES


1. L. Escalada, J. Lutz, S.P. Brühl, M. Fazio, A. Márquez, S. Mändl, D. Manova, S.N. Simison. Microstructure and corrosion behavior of AISI 316L duplex treated by means of ion nitriding and plasma based ion implantation and deposition // *Surface and Coatings Technology*. 2013, v. 223, p. 41-46.
2. Y. Sun, T. Bell. Combined Plasma Nitriding and PVD Treatments // *Transaction Inst. of Met. Finishing*. 1992, v. 70(1), p. 38-44.
3. V.A. Belous, I.G. Yermolenko, Yu.A. Zadneprovsky, N.S. Lomino. Combined vacuum-arc hardening of frictional unit components // *Problems of Atomic Science and Technology.* 2016, N 4 (104), p. 93-99.
4. N.A. Dolgov, A.V. Rutkovskyi. Structural steel microhardness improvement by ion nitriding // *Strength of Materials*. 2022, v. 54, N 5, p. 819-824.
5. J. Vetter, W. Burgmer, A.J. Perry. Arc-enhanced glow discharge in vacuum arc machines // *Surface and Coatings Technology*. 1993, v. 59, p. 152-155.
6. V. Gorokhovsky, P. Del Bel Belluz. Ion treatment by low pressure arc plasma immersion surface engineering processes // *Surface and Coatings Technology*. 2013, v. 215, p. 431-439.
7. B. Warcholinski, A. Gilewicz, M. Tarnowska. The Surface Assessment and the Properties of Selected Multilayer Coatings // *Lubricants*. 2023, v. 11(9), p. 371.
8. M. Szala, M. Walczak, K. Pasierbiewicz, M. Kami´nski. Cavitation Erosion and SlidingWear Mechanisms of AlTiN and TiAlN Films Deposited on Stainless Steel Substrate // *Coatings.* 2019, v. 9, p. 340; doi:10.3390/coatings9050340
9. J. Gerth, U. Wiklund. The influence of metallic interlayers on the adhesion of PVD TiN coatings on high-speed steel // *Wear*. 2008, v. 264, p. 885-892.
10. В.А. Белоус, Ю.А. Заднепровский, Н.С. Ломино, И.С. Домнич, С.В. Худяков. Влияние обработки поверхности стали бомбардирующими ионами на ее твердость и глубину азотирования // *Материалы 13-й Международной научно-технической конференции «Взаимодействие излучения с твердым телом».* Беларусь, Минск, 30 сентября – 3 октября 2019 г., с. 213-217.
11. V.A. Belous, Yu.A. Zadneprovsky, I.S. Domnich. Influence of surface pre-heating on the nitriding depth of steel 25CrMoV used complex ion-plasma treatment // *Problems of Atomic Science and Technology*. 2021, v. 135(5), p. 115-121.
12. I.O. Klimenko, V.G. Marinin, V.A. Belous, N.A. Azarenkov, M.G. Ishchenko, V.S. Goltvyanytsya, A.S. Kuprin. Cavitation erosion resistance of vacuum-arc coating based on TiN // *Problems of Atomic Science and Technology*. 2023, v. 147(5), p. 126-136.
13. V.A. Belous, Y. Zadneprovskiy, M. Lomino, I. Domnich, T.I. Bevs. Influence of ionic bombardment on the processes of nitriding during complex modification of steel surface // *East European Journal of Physics*. 2018, v. 4, p. 98-102.
14. B. Schwarz, H. Gohring, S.R. Meka, et al. Pore Formation Upon Nitriding Iron and Iron-Based Alloys: The Role of Alloying Elements and Grain Boundaries // *The Minerals, Metals and Materials Society and ASM International.* 2014.
15. A. Krella. Resistance of PVD coatings to erosive and wear processes: A Review // *Coatings*. 2020, v. 10(10), p. 921.
16. V. Safonov, A. Zykova, J. Steller, G. Tolmachova, N. Donkov. Effect of carbon content on resistance to cavitation erosion of Cr-C coatings deposited by Arc PVD method // *Journal of Physics: Conference Series*. 2023, v. 2487(1), p. 012034.
17. A.K. Krella. Degradation and Protection of Materials from Cavitation Erosion: A Review // *Materials*. 2023, v. 16(5), p. 2058.
18. A. Gilewicz, B. Warcholinski, D. Murzynski. The properties of molybdenum nitride coatings obtained by cathodic arc evaporation // *Surface and Coatings Technology*. 2013, v. 236, p. 149-158.
19. A. Krella. Cavitation erosion of TiN and CrN coatings deposited on different substrates // *Wear*. 2013, v. 297(1-2), p. 992-997.
20. I.O. Klimenko, V.G. Marinin, V.D. Ovcharenko, V.I. Kovalenko, A.S. Kuprin, O.M. Reshetnyak, V.A. Belous, H.Yu. Rostova. Resistance of titanium alloys to cavitation wear // *Problems of Atomic Science and Technology*. 2022, N 1(137), p. 130-135.


*Article received 20.03.2024*

## ВПЛИВ МЕТАЛЕВОГО ПІДШАРУ НА КАВІТАЦІЙНУ СТІЙКІСТЬ АЗОТОВАНОЇ СТАЛІ З ПОКРИТТЯМ $Mo_2N$

***Ю.А. Задніпровський, В.А. Білоус, І.С. Домнич, В.І. Коваленко, Г.Ю. Ростова, І.Г. Танцюра, Г.М. Толмачова, М.Г. Іщенко, О.С. Купрін***

Проведено комплексне модифікування сталі 25CrMoV, що включає азотування у плазмі двоступеневого вакуумно-дугового розряду, осадження металевого підшару (Mo, Cr або Ti) і верхнього шару $Mo_2N$-покриття. Дослідження структури показали, що залежно від матеріалу і товщини підшару (1,5...6 мкм) на межах розділу можуть формуватися дефекти і розшарування, а без металевого підшару дефекти відсутні. Концентрація азоту в комплексно-модифікованих шарах залежить від складу металевого підшару, але не впливає на загальну глибину зміцненої азотуванням сталі ~ 160 мкм. Твердість азотованого шару становить ~ 12 ГПа, а твердість покриття $Mo_2N$ ~ 30 ГПа. Кавітаційна стійкість комплексно-модифікованої сталі 25CrMoV без металевого підшару у 2 рази вища за сталь у вихідному стані.